An Evaluation of Feature Matchers for Fundamental Matrix Estimation

Jia-Wang Bian[1,2]
jiawang.bian@adelaide.edu.au
Yu-Huan Wu[3]
wuyuhuan@mail.nankai.edu.cn
Ji Zhao[4]
ji.zhao@tusimple.ai
Yun Liu[3]
nk12csly@mail.nankai.edu.cn
Le Zhang[5]
zhangleuestc@gmail.com
Ming-Ming Cheng[3]
cmm@nankai.edu.cn
Ian Reid[1,2]
ian.reid@adelaide.edu.au

[1] School of Computer Science, The University of Adelaide, Adelaide, Australia
[2] Australian Centre for Robotic Vision, Australia
[3] Nankai University, China
[4] TuSimple, China
[5] Agency for Science, Technology and Research, Singapore

Abstract

Matching two images while estimating their relative geometry is a key step in many computer vision applications. For decades, a well-established pipeline, consisting of SIFT, RANSAC, and 8-point algorithm, has been used for this task. Recently, many new approaches were proposed and shown to outperform previous alternatives on standard benchmarks, including the learned features, correspondence pruning algorithms, and robust estimators. However, whether it is beneficial to incorporate them into the classic pipeline is less-investigated. To this end, we are interested in **i)** evaluating the performance of these recent algorithms in the context of image matching and epipolar geometry estimation, and **ii)** leveraging them to design more practical registration systems. The experiments are conducted in four large-scale datasets using strictly defined evaluation metrics, and the promising results provide insight into which algorithms suit which scenarios. According to this, we propose three high-quality matching systems and a Coarse-to-Fine RANSAC estimator. They show remarkable performances and have potentials to a large part of computer vision tasks. To facilitate future research, the full evaluation pipeline and the proposed methods are made publicly available.

1 Introduction

Matching two images while recovering their geometric relation, *e.g.*, *epipolar geometry* [17], is one of the most basic tasks in computer vision and a crucial step in many applications such as Structure-from-Motion (SfM) [1, 20, 32, 37, 38] and Visual SLAM [11, 15, 31]. In these

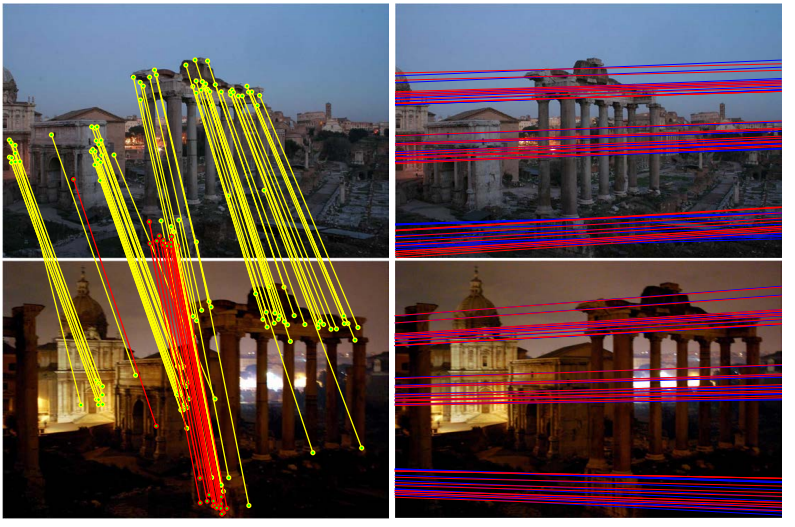

(a) Matching (%Inlier: 78.41) (b) Estimation (NSGD: 0.0046)

Figure 1: Outputs of the two-view matching and geometry estimation pipeline. (a) shows matching results with yellow/red lines standing for inliers/outliers. (b) shows epipolar geometry estimation results with red/blue lines standing for the ground-truth/estimated epipolar lines. We use the proposed *normalized symmetric geometric distance* (NSGD) to measure the estimation accuracy. The smaller, the better.

applications, the overall performance heavily depends on the quality of the initial two-view registration. Consequently, a thorough performance evaluation for this module is of vital importance to the computer vision community. However, to the best of our knowledge, no previous work has done it. To this end, we are dedicated to an extensive experimental evaluation of existing algorithms to establish a uniform evaluation protocol in this paper.

For decades, a classic pipeline has been used for this task, which relies on the SIFT [24] features to establish initial correspondences across images, then prunes bad correspondences by Lowe's *ratio test* [24], and finally estimates the geometry using RANSAC [14] based estimators. We are here interested in recovering the *fundamental matrix* (FM), which suits more general scenes than other geometric models, *e.g.*, the *homography* and *essential matrix*. Fig. 1 shows an example output of this pipeline. Here, we mainly focus on the geometry estimation quality.

Recently, many new approaches were proposed which showed potentials to this task, including the learned features [25, 29, 30], robust estimators [6, 34], and, especially, correspondence pruning algorithms [7, 26, 47] which revived comparatively little attention over before. However, while these algorithms outperform earlier ones on standard benchmarks, incorporating them into the classic pipeline may not necessarily translate into a performance increase. For example, Balntas *et al.* [4] showed that descriptors which perform better than others on the standard benchmark [8] do not show a better image matching quality. The inconsistency was also shown and discussed in [7, 39, 47].

In this paper, we conduct a comprehensive evaluation of recently proposed algorithms by incorporating them into the well-established image matching and epipolar geometry estimation pipeline to investigate whether they can increase the overall performance. In detail,

this paper makes the following contributions:

- **i)** We present an evaluation protocol for local features, robust estimators, and especially correspondence pruning algorithms such as [7, 26, 47] which have not been carefully investigated.
- **ii)** We evaluate algorithms on four large-scale datasets using strictly defined metrics. The results provide insights into which datasets are particularly challenging and which algorithms suit which scenarios.
- **iii)** Based on the results, we propose three high-quality and efficient matching systems, which perform on par with the powerful CODE [23] system but are several orders of magnitude faster.
- **iv)** Interestingly, we observe that the recent GC-RANSAC [6] (also USAC [34]) does not show consistently high performance on geometry estimation but permits effective outlier pruning. We hence propose to first use it for outlier removal, and then apply LMedS based estimator [36] for model fitting. The resulting approach, termed Coarse-to-Fine RANSAC, shows significant superiority over other alternatives.

2 Related work

Rich research focuses on evaluating local features and robust estimators, while correspondence pruning algorithms have not been well evaluated. The proposed benchmark mitigates this gap.

Evaluating Local Features. Mikolajczyk *et al.* [28] evaluated the affine region detectors on small-scale datasets, which cover various photometric and geometric image transformations. Later, Mikolajczyk and Schmid [27] extended the evaluation to local descriptors. Build upon this, Heinly *et al.*[19] proposed several additional metrics and datasets to evaluate binary descriptors. Besides, Brown *et al.* [8] presented a patch pair classification benchmark for the learned descriptors, which measures the ability of a descriptor to discriminate positive from negative patch pairs. Recently, Balntas *et al.*[5] evaluated the hand-crafted and learned descriptors in terms of the verifying and retrieving *homography* patches. Schönberger *et al.*[39] comparatively evaluated these two types of descriptors in the context of image-based reconstruction.

Evaluating Robust Estimators. Choi *et al.*[10] conducted an evaluation of RANSAC [14] family in terms of the line fitting and homography estimation [17], where the accuracy, runtime, and robustness of methods are analyzed. Lacey *et al.*[22] performed an evaluation of RANSAC algorithms for stereo camera calibration. Raguram *et al.*[33] categorized RANSAC algorithms and provide a comparative analysis on them, where the trade-off between efficiency and accuracy is considered. These protocols evaluate robust model fitting techniques in both synthetic and real data. Torr *et al.* [42, 44] provided performance characterization of *fundamental matrix* (FM) estimation algorithms. Zhang [48] reviewed FM estimation techniques and proposed a well-founded measure to compute the distance of two fundamental matrices, which is shown to better than using the Frobenius norm. Armanguè *et*

Algorithm 1 Compute SGD

Input: I_1, I_2, F_1, F_2, N
Output: sgd
1: **function** COMPUTESGD(I_1, I_2, F_1, F_2, N)
2: $sgd \leftarrow 0$
3: $count \leftarrow 0$
4: **while** $count < N$ **do**
5: randomly choose a point m in I_1
6: draw $l_1 = F_1 m$ in I_2
7: **if** l_1 does not intersect with I_2 **then**
8: continue
9: **end if**
10: randomly choose a point m' on L_1
11: draw $l_2 = F_2 m$ in I_2
12: d'_1 = distance(m', l_2)
13: draw $l_3 = F_2^T m'$ in I_1
14: d_1 = distance(m, l_3)
15: $sgd \leftarrow sgd + d'_1 + d_1$
16: $count \leftarrow count + 1$
17: **end while**
18: swap (I_1, I_2), swap (F_1, F_2)
19: repeat step $3 - 17$
20: $sgd \leftarrow sgd/(4 * N)$
21: **return** sgd
22: **end function**

al. [3] provided an overview on different FM estimation approaches. Fathy *et al.* [13] studied the error criteria in FM estimation phase.

Proposed Benchmark. Our benchmark is mainly motivated by [39] which evaluates descriptors in higher-level tasks. The difference is that we evaluate three types of algorithms in the context of two-view image matching and geometry estimation for the overall performance, while [39] evaluates descriptors in multiple tasks for the generalized descriptor. Besides, we draw from [6, 35, 39, 42, 48] to design the evaluation metric and construct the benchmark dataset. Moreover, the presented evaluation could also be interpreted as an ablation study for image matching and geometry estimation pipeline. It can help researchers design more practical correspondence systems.

3 Evaluation metrics

3.1 Metrics on FM estimation

Fundamental matrices cannot be compared directly due to their structures. For measuring the accuracy of estimation, we follow Zhang's method [48], referred as *symmetric geometry distance* (SGD) in this paper. It generates virtual correspondences using the ground-truth FM and computes the *epipolar distance* to the estimated one, and then reverts their roles to compute the distance again to ensure symmetry. The averaged distance is used for accuracy measurement. Alg. 1 presents an overview for the computation of the SGD error, where (I_1, I_2) is an image pair, F_1 and F_2 are two FMs, and N is the number of maximum iterations.

Normalized SGD. The computed SGD error (*in pixels*) causes comparability issues between images with different resolutions. In order to address this issue, we propose to normalize the distance into the range of $[0, 1]$ by dividing the distance by the length of the image diagonal. Formally, the distance is regularized by multiplying a factor $f = 1/\sqrt{h^2 + w^2}$, where h and w stand for the height and width of the image, respectively. This makes the error comparable across different resolution images.

%Recall. Given the FM estimates, we classify them as accurate or not by thresholding the Normalized SGD error, and use the %Recall, the ratio of accurate estimates to all estimates, for evaluation. In our experiments, 0.05 is used as the threshold. As the recall increasing with thresholds in an accumulative way, the performance is not sensitive to threshold selection. However, we also suggest readers showing recall curves with varying thresholds.

3.2 Metrics on Image Matching

%Inlier. We use the inlier rate, *i.e.*, the ratio of inliers to all matches, to evaluate the correspondence quality. Here, matches whose distance to the ground-truth epipolar line is smaller than certain threshold in both images are regarded as inliers. To avoid the comparability issue caused by different image resolutions, we set the threshold as $\alpha\sqrt{h^2+w^2}$, where h and w are height and width of images, respectively. α is 0.003 in our evaluation. Besides, for analyzing intermediate results, we also report **%Inlier-m**, *i.e.*, the inlier rate before outlier rejection by robust estimators such as RANSAC [14]. This reflects the performance of a pure feature matching system.

#Corrs. We use correspondence numbers for analyzing results rather than performance comparison, since the impact of match numbers to high-level applications such as SfM [37] are arguable [39]. However, too few correspondences would degenerate these applications. Therefore, we pay little attention to match numbers, as long as they are not too small. Similarly, **#Corrs-m**, match numbers before the estimation phase, is also reported.

4 Datasets

We use four large-scale benchmark datasets for evaluation, where different real-world scenes are captured, and camera configurations vary from one to another. Such diversities allow us to compare algorithms in different scenarios.

Datasets. The benchmark datasets include: (1) The TUM SLAM dataset [40], which provides videos of indoor scenes, where the texture is often weak and images are sometimes blurred due to the fast camera movement. (2) The KITTI odometry dataset [16], which consists of consecutive frames in a driving scenario, where the geometry between images is dominated by the forward motion. (3) The Tanks and Temples (T&T) dataset [21], which provides many scans of scenes or objects for image-based reconstruction, and hence offers wide-baseline pairs for evaluation. (4) The Community Photo Collection (CPC) dataset [46], which provides unstructured images of well-known landmarks across the world collected from Flickr. In the CPC dataset, images are taken from arbitrary cameras at a different time. Fig. 2 provides sample images of these benchmark datasets.

Ground Truth. The *fundamental matrix* between an image pair could be derived algebraically from their *projection matrices* ($\mathbf{P}$ and $\mathbf{P}'$) as follows:

$$\mathbf{F} = [\mathbf{P}'\mathbf{C}]_{\times}\mathbf{P}'\mathbf{P}^{+} \tag{1}$$

Figure 2: Sample images from the benchmark datasets.

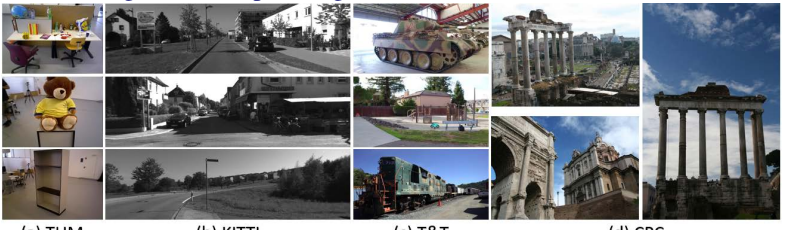

(a) TUM (b) KITTI (c) T&T (d) CPC

Table 1: Details of the benchmark datasets.

Datasets	#Seq	#Image	Resolution	Baseline	Property
TUM	3	5994	480×640	short	indoor scenes
KITTI	5	9065	370×1226	short	street views
T&T	3	922	1080×2048 1080×1920	wide	outdoor scenes
CPC	1	1615	varying	wide	internet photos

where $\mathbf{P}^+$ is the pseudo-inverse of $\mathbf{P}$, *i.e.*, $\mathbf{P}\mathbf{P}^+ = \mathbf{I}$, and $\mathbf{C}$ is a null vector, namely the camera center, defined by $\mathbf{P}\mathbf{C} = \mathbf{0}$. $\mathbf{P} = \mathbf{K}[\mathbf{R}|\mathbf{t}]$ is a 3x4 matrix, and it satisfies

$$d \begin{pmatrix} u \\ v \\ 1 \end{pmatrix} = \mathbf{P} \begin{pmatrix} x \\ y \\ z \\ 1 \end{pmatrix} \tag{2}$$

where d is an unknown depth, $[u, v]$ is the image coordinates, and $[x, y, z]$ is the real-world coordinates. $\mathbf{K}$ is the camera intrinsics, and $[\mathbf{R}|\mathbf{t}]$ is the camera extrinsics. The ground-truth camera intrinsic and extrinsic parameters are provided in TUM and KITTI datasets, while they are unknown in T&T and CPC datasets. Therefore, we derive ground-truth camera parameters for them by reconstructing image sequences using the COLMAP [37], as in [35, 47]. Note that SfM pipeline reasons globally about the consistency of 3D points and cameras, leading to accurate estimates with an average reprojection error below one pixel [37].

Image Pairs Construction. We search for matchable image pairs by identifying inlier numbers, *i.e.*, we generate correspondences across two images using SIFT [24] and choose pairs which contain more than 20 inliers, as in [35]. For wide-baseline datasets (T&T [21] and CPC [46]), all image pairs are searched. For short-baseline datasets (TUM [40] and KITTI [16]), a frame is paired to the subsequent frames captured within one second because almost other pairs are of no overlap. In this way, we obtain a large number of matchable image pairs, and we randomly choose 1000 pairs in each dataset for testing. The testing split on each dataset is described as follows. In the TUM [40] dataset, we test methods on three sequences: *fr3/teddy*, *fr3/large_cabinet*, and *fr3/long_office_household*. In the KITTI [16] Odometry dataset, sequences 06-10 are used. In the T&T [21] dataset, sequences *Panther*, *Playground*, and *Train* are used. In the CPC [46] dataset, *Roman Forum* is used. Other image sequences could be used as training data for further deep learning based methods. Tab. 1 summarizes the test set that we use for evaluation.

5 Experiments

Related research is quite rich, so we mainly focus on evaluating recently proposed algorithms and the widely used methods in this paper. In the following, we introduce the experimental configuration, discuss results, and propose our methods.

5.1 Experimental Setup

Baseline and Comparability. We set a classic pipeline as the baseline. Specifically, we use DoG [24] detector and SIFT [24] descriptor to generate initial correspondences across images by the plain nearest-neighbor search, then prune bad correspondences using Lowe's *ratio test* [24], and finally compute FM estimates and remove outliers using RANSAC [14] with the 8-point algorithm [18]. For each evaluated algorithm, we incorporate it into the baseline system by replacing its counterpart, and use the overall performance for comparison.

Evaluated Methods. Firstly, we evaluate four deep learning based local features, including HesAffNet [30] detector and two descriptors (L2Net [41], HardNet++ [29]). Besides, two hand-crafted descriptors (DSP-SIFT [12] and RootSIFT-PCA [2, 9]) are also evaluated, which show high performance in the recent benchmark [39]. Secondly, we evaluate four correspondence pruning algorithms: CODE [23], GMS [7], LPM [26], and LC [47]. Finally, we evaluate two widely used estimators (LMedS [36] and MSAC [43]) and two state-of-the-art alternatives (USAC [34] and GC-RANSAC [6]).

Implementations. We use VLFeat [45] library for the implementation of SIFT descriptor and DoG detector, and the threshold is 0.8 for *ratio test* [24]. Matlab functions are used for RANSAC, LMedS, and MSAC implementations, where we limit the maximum iteration as 2000 for a reasonable speed. Other codes are from authors' publicly available implementation, where we use the pre-trained models released by authors for deep learning based methods.

5.2 Results and Discussion

Tab. 2 reports the experimental results for all methods and datasets. In each block, the first line shows the baseline performance. First, second, third best results are highlighted in color, and the results that are better than the baseline are highlighted in bold. Here, we mainly compare algorithms in terms of *%Recall*, which reflects the overall performance. In addition, *%Inlier* shows matching performance, and *%Inlier-m* shows matching before outlier rejection phase. *#Corrs(-m)* is used to analyze results instead of performance comparison. The detail about these metrics can be seen in Sec. 3. For performance analyses, we mainly target on concluding the distinctive properties of the best methods instead of a comprehensive comparison of all approaches.

Local Features. Tab. 2(a) shows the results of local features. The *%Recall* implies that **a)** RootSIFT-PCA [9] and HardNet++ [29] consistently outperform the baseline, and the latter is better than the former. **b)** HesAffNet [30] performs best in wide-baseline scenarios (T&T and CPC), although it is degenerate on the TUM dataset. **c)** DSP-SIFT [12] outperforms the

Table 2: Experimental results. First, second, third best results are highlighted in color, and the results that are better than the baseline (the first line in each block) performance are highlighted in bold. %Recall represents the overall performance.

Datasets	(a) Local Features					(b) Pruning Methods					(c) Robust Estimators				
	Methods	%Recall	%Inlier	%Inlier-m	#Corrs (-m)	Methods	%Recall	%Inlier	%Inlier-m	#Corrs (-m)	Methods	%Recall	%Inlier	%Inlier-m	#Corrs (-m)
TUM	SIFT	57.40	75.33	59.21	65 (316)	RATIO	57.40	75.33	59.21	65 (316)	RANSAC	57.40	75.33	59.21	65 (316)
	DSP-SIFT	53.90	74.89	56.44	66 (380)	GMS	**59.20**	**76.18**	**69.72**	64 (241)	LMedS	**69.20**	75.24	59.21	158 (316)
	RootSIFT-PCA	**58.90**	**75.65**	**62.22**	67 (306)	LPM	**58.90**	**75.75**	**64.42**	67 (290)	MSAC	52.70	75.12	59.21	63 (316)
	L2Net	**58.10**	**75.49**	**59.26**	66 (319)	LC	54.10	**75.96**	**71.32**	57 (203)	USAC	**56.50**	72.13	59.21	244 (316)
	HardNet++	**58.90**	**75.74**	**62.07**	67 (315)	CODE	**62.50**	**76.95**	**66.82**	3119 (18562)	GC-RSC	30.80	68.13	59.21	272 (316)
	HesAffNet	51.70	**75.70**	**62.06**	101 (657)										
KITTI	SIFT	91.70	98.20	87.40	154 (525)	RATIO	**91.70**	98.20	87.40	154 (525)	RANSAC	**91.70**	**98.20**	**87.40**	154 (525)
	DSP-SIFT	**92.00**	**98.22**	**87.60**	153 (572)	GMS	**91.70**	**98.58**	**95.56**	148 (445)	LMedS	**91.80**	**98.25**	**87.40**	263 (525)
	RootSIFT-PCA	**92.00**	**98.23**	**90.76**	156 (514)	LPM	91.50	**98.27**	**92.50**	157 (501)	MSAC	**91.80**	**98.12**	**87.40**	153 (525)
	L2Net	91.60	**98.21**	**89.40**	156 (520)	LC	89.70	**99.44**	**97.49**	96 (267)	USAC	82.70	97.39	87.40	455 (525)
	HardNet++	**92.00**	**98.21**	**91.25**	159 (535)	CODE	**92.50**	**98.32**	**93.03**	4834 (19246)	GC-RSC	56.50	95.00	87.40	487 (525)
	HesAffNet	90.40	98.09	**90.64**	233 (1182)										
T&T	SIFT	70.00	75.20	53.25	85 (795)	RATIO	70.00	75.20	53.25	85 (795)	RANSAC	70.00	75.20	**53.25**	85 (795)
	DSP-SIFT	**75.10**	**80.20**	**60.02**	90 (845)	GMS	**80.90**	**84.38**	**77.65**	90 (598)	LMedS	**83.40**	**77.26**	**53.25**	398 (795)
	RootSIFT-PCA	**77.40**	**80.55**	**61.75**	89 (738)	LPM	**80.70**	**81.62**	**66.98**	90 (667)	MSAC	64.60	73.27	**53.43**	84 (799)
	L2Net	**70.40**	73.76	**57.31**	93 (799)	LC	**76.60**	**84.01**	**72.24**	77 (512)	USAC	**78.80**	**80.98**	53.25	495 (795)
	HardNet++	**79.90**	**81.05**	**63.61**	96 (814)	CODE	**89.40**	**89.14**	**76.98**	782 (9251)	GC-RSC	**80.40**	**78.97**	53.25	612 (795)
	HesAffNet	**82.50**	**84.71**	**70.29**	97 (920)										
CPC	SIFT	29.20	67.14	48.07	60 (415)	RATIO	29.20	67.14	48.07	60 (415)	RANSAC	29.20	67.14	**48.07**	60 (415)
	DSP-SIFT	**35.20**	**76.48**	**56.29**	57 (367)	GMS	**43.00**	**85.90**	**82.37**	59 (249)	LMedS	**44.00**	**75.38**	**48.07**	209 (415)
	RootSIFT-PCA	**38.20**	**78.45**	**59.92**	62 (361)	LPM	**39.40**	**78.17**	**65.98**	60 (310)	MSAC	23.00	62.28	**48.07**	59 (415)
	L2Net	**29.60**	60.22	**50.70**	93 (433)	LC	**39.40**	**83.99**	**72.22**	51 (295)	USAC	**49.70**	**80.38**	48.07	232 (415)
	HardNet++	**40.30**	**76.73**	**62.30**	69 (400)	CODE	**51.00**	**90.16**	**78.55**	696 (5774)	GC-RSC	**53.70**	**81.15**	48.07	269 (415)
	HesAffNet	**47.40**	**84.58**	**72.22**	65 (405)										

baseline on almost all datasets but TUM, and L2Net [41] shows similar performances with the baseline on all datasets.

Correspondence Pruning Methods. Tab. 2(b) shows the results of pruning methods. It shows that **a)** CODE [23] achieves the state-of-the-art performance on all datasets. **b)** GMS [7] and LPM [26] consistently outperform the baseline methods by pruning bad correspondences effectively, *i.e.*, improving the *%Inlier-m* and preserving a considerable *#Corrs-m* in the meanwhile. Here, GMS is better than LPM. **c)** LC [47] can boost the matching accuracy (%Inlier-m) but, for estimation (*%Recall*), it is degenerate on the short-baseline datasets (TUM and KITTI). Perhaps this is because the provided model is trained on wide-baseline datasets. Also, note that it requires camera intrinsics, which are normally assumed to be unknown for the FM estimation problem.

Robust Estimators. Tab. 2(c) shows the results of robust estimators. They show: **a)** LMedS [36] performs best on the first three datasets where images are not as difficult as CPC dataset. This confirms the suggestion by Matlab documentation that LMedS works well when the inlier rate is high enough, *e.g.*, above 50%. **b)** GC-RANSAC [6] and USAC [34] show high performances in wide-baseline scenarios, especially on the challenging CPC dataset. However, they are degenerate in short-baseline scenarios (TUM and KITTI). **c)** Interestingly, we observe that GC-RANSAC (also USAC) can preserve rich correspondences (*%Corrs-m*) and prune outliers (*%Inlier(-m)*) effectively.

Runtime. As algorithms rely on different operating systems, we use two machines for evaluation: a Linux server **L** (Intel E5-2620 CPU, NVIDIA Titan Xp GPU) and a Windows laptop **W** (Intel i7-3630QM CPU, NVIDIA GeForce GT 650M GPU), where 100 images

Table 3: Time consumption of evaluated algorithms.

Device	Runtime (seconds)					
L	SIFT	DSP-SIFT	RootSIFT-PCA	L2Net	HardNet++	HesAffNet
	0.702	1.762	0.705	2.260	0.002	0.367
W	LPM	GMS	LC	CODE		
	0.003	0.001	0.021	4.068		
	RANSAC	LMedS	MSAC	USAC	GC-RSC	
	0.521	0.528	0.537	0.565	0.788	

from the KITTI dataset are used for testing and the averaged results are reported. Tab. 3 reports the time consumption of algorithms. Descriptors rely on DoG [24] detector, which (**L**) takes 238*ms* to extract 1760 keypoints, and HesAffNet [30] detector extracts 4860 keypoints. CODE [23] (**W**) takes 2.953*s* to extract 58,675 keypoints using GPU, and takes 4.068*s* to prune bad correspondences using CPU.

5.3 Proposed Methods

Drawing inspiration from the results, we propose three practical matching systems and a robust estimator as follows.

Matching Systems. We first adopt one of the following three pairs of detectors and descriptors for generating putative correspondences:

1. DoG [24] + RootSIFT-PCA [9]
2. DoG + (HardNet++) [29]
3. HesAffNet [30] + (HardNet++)

where we recommend 1, 2 for general scenes and 3 for wide-baseline scenarios. Then, we apply *ratio test* (the threshold is 0.8) and GMS [7] to prune bad correspondences. Finally, we use LMedS [36] based estimator for model fitting. Tab. 4 shows the evaluation results, which clearly demonstrate that the recommended systems outperform the baseline, and achieve competitive performances with the state-of-the-art system (CODE [23] + LMedS [36]). Note that CODE is several orders of magnitude slower, even GPU is adopted.

Coarse-to-Fine RANSAC. Tab. 2 shows that GC-RANSAC [6] and USAC [34] prune outliers effectively, although they fail to show consistently high performance on model fitting. To this end, we propose to use GC-RANSAC [6] for pruning bad matches, and then apply LMedS [36] based estimator for model fitting. Note that USAC is also applicable. In this two-stage framework, the former is used to roughly find the inlier set and the latter to fit the model accurately, so we term the resultant approach Coarse-to-Fine RANSAC (CF-RSC in short). Tab. 5 shows the results of the proposed method in terms of *%Recall*, where all estimators use the same input, *i.e.*, SIFT [24] matches with *ratio test* pruning. It shows that the proposed CF-RSC significantly outperforms other alternatives.

6 Conclusions

Table 4: Evaluation results of the proposed matching systems.

Datasets	Methods	%Recall	%Inlier	%Inlier-m	#Corrs(-m)
TUM	Baseline	57.40	75.33	59.21	65 (316)
	CODE	**67.50**	**76.04**	**66.82**	9281 (18562)
	RootSIFT-PCA + GMS	**67.50**	**76.13**	**69.62**	124 (248)
	HardNet + GMS	**68.60**	**75.85**	**69.39**	128 (256)
	HesAffNet + GMS	**66.40**	**75.92**	**67.04**	288 (577)
KITTI	Baseline	91.70	98.20	87.40	154 (525)
	CODE	**91.90**	**98.22**	**93.03**	9623 (19246)
	RootSIFT-PCA + GMS	**92.50**	**98.54**	**95.73**	225 (450)
	HardNet + GMS	**92.10**	**98.49**	**95.43**	236 (472)
	HesAffNet + GMS	**91.80**	**98.48**	**94.18**	540 (1079)
T&T	Baseline	70.00	75.20	53.25	85 (795)
	CODE	**92.70**	**87.81**	**76.98**	4626 (9251)
	RootSIFT-PCA + GMS	**89.30**	**85.29**	**78.69**	307 (614)
	HardNet + GMS	**92.20**	**85.52**	**78.86**	343 (686)
	HesAffNet + GMS	**90.90**	**86.16**	**79.25**	412 (824)
CPC	Baseline	29.20	67.14	48.07	60 (415)
	CODE	**61.80**	**89.45**	**78.55**	2890 (5774)
	RootSIFT-PCA + GMS	**57.30**	**88.94**	**83.70**	133 (263)
	HardNet + GMS	**60.10**	**88.34**	**83.12**	149 (298)
	HesAffNet + GMS	**60.80**	**88.72**	**83.16**	182 (362)

Table 5: %Recall of the proposed CF-RSC.

Datasets	RANSAC	LMedS	MSAC	USAC	GC-RSC	CF-RSC
TUM	57.40	69.20	52.70	56.50	30.80	**69.30**
KITTI	91.70	91.80	91.80	82.70	56.50	**92.30**
T&T	70.00	83.40	64.60	78.80	80.40	**90.70**
CPC	29.20	44.00	23.00	49.70	53.70	**60.90**

This paper evaluates the recently proposed local features, correspondence pruning algorithms, and robust estimators using strictly defined metrics in the context of image matching and fundamental matrix estimation. Comprehensive evaluation results on four large-scale datasets provide insights into which datasets are particularly challenging and which algorithms perform well in which scenarios. This can advance the development of related research fields, and it can also help researchers design practical matching systems in different applications. Finally, drawing inspiration from the results, we propose three high-quality image matching systems and a robust estimator, Coarse-to-Fine RANSAC. They achieve remarkable performances and have potentials in a wide range of computer vision tasks.

7 Acknowledgement

The authors would like to thank TuSimple and Huawei Technologies Co. Ltd.

References

[1] Sameer Agarwal, Yasutaka Furukawa, Noah Snavely, Ian Simon, Brian Curless, Steven M Seitz, and Richard Szeliski. Building Rome in a day. *Communications of the ACM*, 54(10):105–112, 2011.

[2] Relja Arandjelovic and Andrew Zisserman. Three things everyone should know to improve object retrieval. In *IEEE Conference on Computer Vision and Pattern Recognition (CVPR)*, pages 2911–2918. IEEE, 2012.

[3] Xavier Armangué and Joaquim Salvi. Overall view regarding fundamental matrix estimation. *Image and Vision Computing*, 21(2):205–220, 2003.

[4] Vassileios Balntas, Edgar Riba, Daniel Ponsa, and Krystian Mikolajczyk. Learning local feature descriptors with triplets and shallow convolutional neural networks. In *British Machine Vision Conference (BMVC)*, page 3, 2016.

[5] Vassileios Balntas, Karel Lenc, Andrea Vedaldi, and Krystian Mikolajczyk. HPatches: A benchmark and evaluation of handcrafted and learned local descriptors. In *IEEE Conference on Computer Vision and Pattern Recognition (CVPR)*, pages 5173–5182. IEEE, 2017.

[6] Daniel Barath and Jiri Matas. Graph-Cut RANSAC. In *IEEE Conference on Computer Vision and Pattern Recognition (CVPR)*, 2018.

[7] JiaWang Bian, Wen-Yan Lin, Yasuyuki Matsushita, Sai-Kit Yeung, Tan Dat Nguyen, and Ming-Ming Cheng. GMS: Grid-based motion statistics for fast, ultra-robust feature correspondence. In *IEEE Conference on Computer Vision and Pattern Recognition (CVPR)*, pages 4181–4190. IEEE, 2017.

[8] Matthew Brown, Gang Hua, and Simon Winder. Discriminative learning of local image descriptors. *IEEE Transactions on Pattern Recognition and Machine Intelligence (PAMI)*, pages 43–57, 2011.

[9] Andrei Bursuc, Giorgos Tolias, and Hervé Jégou. Kernel local descriptors with implicit rotation matching. In *International Conference on Multimedia Retrieval*, pages 595–598. ACM, 2015.

[10] Sunglok Choi, Taemin Kim, and Wonpil Yu. Performance evaluation of RANSAC family. *International Journal on Computer Vision (IJCV)*, 24(3):271–300, 1997.

[11] Andrew J Davison, Ian D Reid, Nicholas D Molton, and Olivier Stasse. MonoSLAM: Real-time single camera slam. *IEEE Transactions on Pattern Recognition and Machine Intelligence (PAMI)*, 29(6):1052–1067, 2007.

[12] Jingming Dong and Stefano Soatto. Domain-size pooling in local descriptors: DSP-SIFT. In *IEEE Conference on Computer Vision and Pattern Recognition (CVPR)*, pages 5097–5106, 2015.

[13] Mohammed E Fathy, Ashraf S Hussein, and Mohammed F Tolba. Fundamental matrix estimation: A study of error criteria. *Pattern Recognition Letters*, 32(2):383–391, 2011.

[14] Martin A Fischler and Robert C Bolles. Random sample consensus: a paradigm for model fitting with applications to image analysis and automated cartography. *Communications of the ACM*, 24(6):381–395, 1981.

[15] Christian Forster, Matia Pizzoli, and Davide Scaramuzza. SVO: Fast semi-direct monocular visual odometry. In *International Conference on Robotics and Automation (ICRA)*, pages 15–22. IEEE, 2014.

[16] Andreas Geiger, Philip Lenz, and Raquel Urtasun. Are we ready for autonomous driving? the KITTI vision benchmark suite. In *IEEE Conference on Computer Vision and Pattern Recognition (CVPR)*, pages 3354–3361. IEEE, 2012.

[17] Richard Hartley and Andrew Zisserman. *Multiple view geometry in computer vision*. Cambridge university press, 2003.

[18] Richard I Hartley. In defense of the eight-point algorithm. *IEEE Transactions on Pattern Recognition and Machine Intelligence (PAMI)*, 19(6):580–593, 1997.

[19] Jared Heinly, Enrique Dunn, and Jan-Michael Frahm. Comparative evaluation of binary features. In *European Conference on Computer Vision (ECCV)*, pages 759–773. Springer, 2012.

[20] Jared Heinly, Johannes L Schonberger, Enrique Dunn, and Jan-Michael Frahm. Reconstructing the world* in six days*(as captured by the yahoo 100 million image dataset). In *IEEE Conference on Computer Vision and Pattern Recognition (CVPR)*, pages 3287–3295, 2015.

[21] Arno Knapitsch, Jaesik Park, Qian-Yi Zhou, and Vladlen Koltun. Tanks and Temples: Benchmarking large-scale scene reconstruction. *ACM Transactions on Graphics (TOG)*, 36(4):78, 2017.

[22] AJ Lacey, N Pinitkarn, and Neil A Thacker. An evaluation of the performance of RANSAC algorithms for stereo camera calibrarion. In *British Machine Vision Conference (BMVC)*, pages 1–10, 2000.

[23] Wen-Yan Lin, Fan Wang, Ming-Ming Cheng, Sai-Kit Yeung, Philip HS Torr, Minh N Do, and Jiangbo Lu. CODE: Coherence based decision boundaries for feature correspondence. *IEEE Transactions on Pattern Recognition and Machine Intelligence (PAMI)*, 2017.

[24] David G Lowe. Distinctive image features from scale-invariant keypoints. *International Journal on Computer Vision (IJCV)*, 60(2):91–110, 2004.

[25] Zixin Luo, Tianwei Shen, Lei Zhou, Siyu Zhu, Runze Zhang, Yao Yao, Tian Fang, and Long Quan. GeoDesc: Learning local descriptors by integrating geometry constraints. In *European Conference on Computer Vision (ECCV)*, 2018.

[26] Jiayi Ma, Ji Zhao, Junjun Jiang, Huabing Zhou, and Xiaojie Guo. Locality preserving matching. *International Journal on Computer Vision (IJCV)*, 2018.

[27] Krystian Mikolajczyk and Cordelia Schmid. A performance evaluation of local descriptors. *IEEE Transactions on Pattern Recognition and Machine Intelligence (PAMI)*, 27 (10):1615–1630, 2005.

[28] Krystian Mikolajczyk, Tinne Tuytelaars, Cordelia Schmid, Andrew Zisserman, Jiri Matas, Frederik Schaffalitzky, Timor Kadir, and Luc Van Gool. A comparison of affine region detectors. *International Journal on Computer Vision (IJCV)*, 65(1-2):43–72, 2005.

[29] Anastasiia Mishchuk, Dmytro Mishkin, Filip Radenovic, and Jiri Matas. Working hard to know your neighbor's margins: Local descriptor learning loss. In *Neural Information Processing Systems (NIPS)*, pages 4826–4837, 2017.

[30] Dmytro Mishkin, Filip Radenovic, and Jiri Matas. Repeatability is not enough: Learning affine regions via discriminability. In *European Conference on Computer Vision (ECCV)*. Springer, 2018.

[31] Raul Mur-Artal, Jose Maria Martinez Montiel, and Juan D Tardos. ORB-SLAM: a versatile and accurate monocular slam system. *IEEE Transactions on Robotics (TRO)*, 31(5):1147–1163, 2015.

[32] Filip Radenovic, Johannes L Schönberger, Dinghuang Ji, Jan-Michael Frahm, Ondrej Chum, and Jiri Matas. From dusk till dawn: Modeling in the dark. In *IEEE Conference on Computer Vision and Pattern Recognition (CVPR)*, pages 5488–5496, 2016.

[33] Rahul Raguram, Jan-Michael Frahm, and Marc Pollefeys. A comparative analysis of RANSAC techniques leading to adaptive real-time random sample consensus. In *European Conference on Computer Vision (ECCV)*, pages 500–513. Springer, 2008.

[34] Rahul Raguram, Ondrej Chum, Marc Pollefeys, Jiri Matas, and Jan-Michael Frahm. USAC: a universal framework for random sample consensus. *IEEE Transactions on Pattern Recognition and Machine Intelligence (PAMI)*, 35(8):2022–2038, 2013.

[35] René Ranftl and Vladlen Koltun. Deep fundamental matrix estimation. In *European Conference on Computer Vision (ECCV)*, pages 284–299, 2018.

[36] Peter J Rousseeuw and Annick M Leroy. *Robust regression and outlier detection*, volume 589. John wiley & sons, 1987.

[37] Johannes L Schönberger and Jan-Michael Frahm. Structure-from-motion revisited. In *IEEE Conference on Computer Vision and Pattern Recognition (CVPR)*, pages 4104–4113, 2016.

[38] Johannes L Schönberger, Filip Radenovic, Ondrej Chum, and Jan-Michael Frahm. From single image query to detailed 3d reconstruction. In *IEEE Conference on Computer Vision and Pattern Recognition (CVPR)*, pages 5126–5134, 2015.

[39] Johannes L Schönberger, Hans Hardmeier, Torsten Sattler, and Marc Pollefeys. Comparative evaluation of hand-crafted and learned local features. In *IEEE Conference on Computer Vision and Pattern Recognition (CVPR)*, pages 6959–6968. IEEE, 2017.

[40] J. Sturm, N. Engelhard, F. Endres, W. Burgard, and D. Cremers. A benchmark for the evaluation of RGB-D SLAM systems. In *IEEE International Conference on Intelligent Robots and Systems (IROS)*, Oct. 2012.

[41] Yurun Tian, Bin Fan, Fuchao Wu, et al. L2-Net: Deep learning of discriminative patch descriptor in euclidean space. In *IEEE Conference on Computer Vision and Pattern Recognition (CVPR)*, volume 1, page 6, 2017.

[42] Philip HS Torr and David W Murray. The development and comparison of robust methods for estimating the fundamental matrix. *International Journal on Computer Vision (IJCV)*, 24(3):271–300, 1997.

[43] Philip HS Torr and Andrew Zisserman. MLESAC: A new robust estimator with application to estimating image geometry. *Computer Vision and Image Understanding (CVIU)*, 78(1):138–156, 2000.

[44] Philip HS Torr and A Zissermann. Performance characterization of fundamental matrix estimation under image degradation. *Machine Vision and Applications*, 9(5-6):321–333, 1997.

[45] Andrea Vedaldi and Brian Fulkerson. VLFeat: An open and portable library of computer vision algorithms. In *ACM International Conference on Multimedia (ACM MM)*, pages 1469–1472. ACM, 2010.

[46] Kyle Wilson and Noah Snavely. Robust global translations with 1DSFM. In *European Conference on Computer Vision (ECCV)*, pages 61–75. Springer, 2014.

[47] Kwang Moo Yi, Eduard Trulls, Yuki Ono, Vincent Lepetit, Mathieu Salzmann, and Pascal Fua. Learning to find good correspondences. In *IEEE Conference on Computer Vision and Pattern Recognition (CVPR)*, 2018.

[48] Zhengyou Zhang. Determining the epipolar geometry and its uncertainty: A review. *International Journal on Computer Vision (IJCV)*, 27(2):161–195, Mar 1998. ISSN 1573-1405. doi: 10.1023/A:1007941100561.